Control of Silicone-Sheathed Electrostatic Clutches for Soft Pneumatic Actuator Position Control

Gregory M. Campbell¹, R. Daelan Roosa¹, Kevin Turner¹, James Pikul², and Mark Yim¹

Abstract—A minimal number of rigid constraints makes soft robots versatile, but many of these robots use soft pneumatic actuators (SPAs) designed to inflate through a single trajectory. In an unloaded actuator, this trajectory is dictated by the arrangement of in-extensible and elastic materials. External strain limiters can be added post-fabrication to SPAs, but these are passive devices. In this paper, we offer design and control techniques for an electrically active strain limiter that is easily adhered to existing SPAs to provide signal-controlled force output. These sheathed electroadhesive (EA) clutches apply antagonistic forces through the constitutive properties of their silicone sheathing and through the variable friction of the clutch itself. We are able to design the sheathing to passively support loads or minimize passive stiffness. We control clutch forces via an augmented pulse-width-modulation (PWM) of the high voltage square-wave input. We perform an initial, empirical characterization on the system with tensile material testing. The clutch system resists motion with sustained forces ranging from 0.5N to 22N. We then demonstrate its ability to apply predictable nonconservative work in a dynamic catching task, where it can limit catching height from 15cm to 1cm. Finally, we attach it to an inverse pneumatic artificial muscle (IPAM) to show that variable strain limitation can control position of the SPA endpoint.

keywords: Soft Robot Materials and Design, Hydraulic/Pneumatic Actuators, Force Control, Electroadhesive clutch

I. Introduction

A soft pneumatic actuator (SPA) often inflates along a single determined range of motion that is prescribed by the design of its material composition [1], [2]. These single-configuration SPAs are fundamentally limited in their ability to controllably adapt to new shapes and actuation modes when they rely on passive inextensible materials, such as fabric [3] or fibers [4], to restrict expansion. If an alternative range of motion is desired, a new actuator must be manufactured or the structure must be manually altered [5].

Other groups have applied antagonistic forces by actively programming the stiffness of surrounding materials [6], [7] or applying external forces such as adding tendons [8]. The resulting systems go through various inflation trajectories depending on the activation of the antagonistic devices and corresponding strain limitation. A trunk-shaped actuator can be converted from a single degree-of-freedom (DoF) to a 3-DoF workspace with the inclusion of three antagonistic materials spaced around its circumference [6].

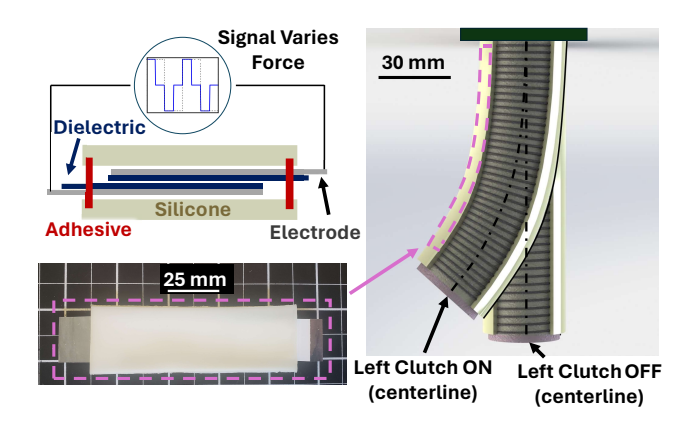


Fig. 1: (left) Silicone-sheathed electrostatic clutch. On-state properties are controlled electronically via pulse-width modulation of high voltage square-wave. System consists of a variable silicone layer connected with Sil-Poxy adhesive to a 50 μm electrode layer of AL-sputtered BOPET with a 25 μm layer of Luxprint dielectric. (right) Antagonistic clutch system attached to the left side of a SPA to provide position control during inflation. Inflation with fully activated clutch superimposed over inflation with deactivated clutch.

External strain limitations often require stiff materials to provide mounting points on the SPA [8]. An alternative approach is to mount the antagonistic components in sleeves, which can distribute the forces along the SPA [9]. Passive sleeves have allowed for significantly varied kinematic behavior [10] and pressure-dependent friction [11]. However without active components, these sleeves have yet to allow for real-time modulation of shape or position.

Electroadhesive (EA) clutches are strong, low-profile components that offer adaptability for soft robots without compromising their flexible nature [12]. EA clutches consume less power than motor-driven tendons, while providing electrical control that is faster and more energy efficient than stiffening approaches that rely on phase change [13]-[15]. They are stronger than fluidic or jamming based solutions, with some clutches holding over 20 Ncm⁻² [15], and avoid complications of additional pumps, compressors, valving, or tubing. However, EA clutches have binary (active/inactive) control authority. While this is valuable to rapidly move between discrete states [12], it is not always useful for applications where force application persists through the extension of the clutches. Force applied during motion utilizes sliding friction force between the clutch plates, and is dependent on the electrostatic force of the clutches. If the clutch force can be modulated, then this sliding friction force is also variable. To

¹Department of Mechanical Engineering and Applied Mechanics (MEAM) at University of Pennsylvania, Philadelphia, PA USA (email: gcampbel@seas.upenn.edu, yim@seas.upenn.edu)

²Department of Mechanical Engineering at University of Wisconsin-Madison, Madison, WI USA

function in this 'variable friction' regime, Hinchet et al. added an additional sliding layer on top of their dielectric and varied the magnitude of their input voltage [16]. However, in another recent work by Feizi et al., [17] a similar effect is achieved by introducing a form of pulse-width-modulation (PWM) into the square-wave input. In this way, the need for an additional sliding layer and change in the magnitude of voltage were avoided. This offloading of complexity from the physical system to the electrical control can also benefit soft systems, which already contain a substantial amount of physical complexity.

EA clutches are sensitive to external contamination and their holding force is reliant on precise orientation. This is often overcome practically by surrounding the soft components with rigid structures to ensure functionality [17]. In applications that rely on fully compliant robots, this is not an option, and instead fabric sleeves have been employed to provided protection and clutch pretension [16]. While fabric sleeves are a natural solution for human interaction, they are not always easy to integrate into SPAs. Siliconebased strain limiters, on the other hand, have been shown to integrate well into silicone-based SPAs [5]. They also allow for design versatility, as silicone can be cast in a wide range of shapes with highly variable thickness to accommodate actuator needs. The Ecoflex used in our system provides superior stretch compared to fabrics, matching the strain of the SPA, while alternative silicones could be used to provide greater rigidity.

This work demonstrates the design and modeling of a sheathed-clutch system that can be easily implemented as an active sleeve for silicone SPAs. These sleeved clutches provide antagonistic tension forces which are varied using PWM of electrical inputs. We demonstrate fabrication strategies for contaminant-resistant EA clutch systems that can be adhered directly to silicone robots. We model the silicone sheathing to choose appropriate stiffness for our applications and use a varied control strategy (similar to [17]) to alter the force-response of our clutch system in real time. We then demonstrate the utility of this clutch system in a dynamic catching task that relates increased clutch force energy dissipation to a reduced displacement throughout the catch. Finally, we demonstrate endpoint position control of a pneumatic prismatic joint actuator.

II. MODELING

Designing a sheathed clutch for specific force applications requires an understanding of the holding forces in both the clutch and the silicone sheathing. Clutches have been well modeled [13], [14], and both fracture and friction models have been used in clutch design [18]. We will assume a friction-based response:

$$F_{clutch} = \frac{\mu \cdot \varepsilon_0 \cdot A}{2} \cdot \left(\frac{\varepsilon_r \cdot V}{d}\right)^2 \tag{1}$$

where μ is the coefficient of friction between clutch pads, d is the distance between the pads, ε_0 is the permittivity of free space, ε_r is the relative permittivity of the EA pad dielectric,

A is the surface area of the electrode, and V is the potential difference between clutch plates.

Modeling hyperelastic elastomers depends on assumptions about both material response and boundary conditions. We will assume a diagonal deformation gradient **F** (only principal stretches $\lambda_1, \lambda_2, \lambda_3$), the incompressibility of silicone and uniaxial expansion ($\lambda = \lambda_1, \lambda_2 = \lambda_3 = \frac{1}{\sqrt{\lambda}}$), and homogeneous, path independent (hyperelastic) expansion. Due to the relatively high stiffnesses of adhesives and clutch plates, we consider stretch only in the length of Ecoflex between adhesives.

Our model uses the Gent strain energy equation [19]: $W = \frac{-\mu J_m}{2} ln(1 - \frac{I_1 - 3}{J_m})$. Where W is the strain energy, μ is the shear modulus, $I_1 = \lambda_1^2 + \lambda_2^2 + \lambda_3^2 = \lambda^2 + 2/\lambda$ is the first invariant (the trace) of the left Cauchy-Green Deformation tensor ($\mathbf{B} = \mathbf{F}\mathbf{F}^T$), and J_m is an empirically solved material property defining the max extension of the molecular chains.

Our assumptions yield the following, simplified, constitutive relations for principal stresses: $\sigma_i = \frac{\delta W}{\delta \lambda_i} \lambda_i + p$. Here p is an undefined hydrostatic pressure responsible for enforcing incompressibility, and \mathbf{I} is the identity matrix. Using the lack of restriction in the non-axial directions of sheath expansion $(\sigma_2 = \sigma_3 = 0)$ to solve for p, the final relation between σ_1 and λ is:

$$\sigma_1 = \frac{\mu J_m}{J_m - I_1 + 3} (\lambda^2 - 1/\lambda)$$
 (2)

With the relationship between stress and stretch fully defined by material properties μ and J_m , the force is dependent on these properties and silicone cross-section area, A: $F_{sheath} = \sigma_{11}A = f(\lambda, \mu, J_m, A)$. Using superposition, we can define the tensile antagonistic force of the sheathed clutch system simply as the following:

$$F_{max} = F_{sheath} + \zeta F_{clutch} \tag{3}$$

where F_{sheath} is fully defined by our design, but F_{clutch} will be controlled via an electrical input varying the variable ζ .

By implementing PWM control, we are able to change ζ from a binary variable to an empirically determined analog value between 0 and 1 and adjust the force response to our needs without altering the electrostatic pressure in Eq. 1.

III. SYSTEM FABRICATION AND CONTROL

The two components of the system, the silicone sheathing and the biaxially-oriented polyethylene terephthalate (BOPET) clutches, are fabricated separately and bonded together with Sil-Poxy silicone adhesive. While we fabricate planar orientations in this work, they also function in a partially curved ('tubular') state similar to [20], as seen when they are adhered to a cylindrical actuator (Fig. 7).

A. Silicone Surface Properties

Platinum-cure silicone can be formed into arbitrary flat shapes with gravity molding, but softer silicones (in, particular EcoFlex 00-30) are relatively tacky, resulting in a high coefficient of friction when sliding along the BOPET backing of an EA clutch. If untreated, this high friction affects off-state stiffness and causes buckling in the clutch plates.

Cornstarch (baby powder) is a commonly used lubricant for silicone systems, and applying it to the contact surface of the silicone greatly reduces this friction. However, EA clutches rely on friction as well, and the presence of powder lubricants contaminates the plates so they can't hold large forces.

Chemical alteration of the silicone surface properties allows for reduced surface friction without negatively affecting clutch performance. Oxidation of the cured silicone followed by fluorination was found to significantly lower the friction coefficient. However, Smooth-On's SLIDE surface diffuser was found to be easier to apply and even more effective. This simple silicone treatment enables the effective use of clutches in contact with the silicone surface. We add 3% by weight of SLIDE to all silicone used for sheathing, and then allow the silicone to rest outside its mold for at least 24 hours prior to adhering clutches. In this work we use 30x100mm rectangles made from 5-10mL of Ecoflex 00-30 per piece.

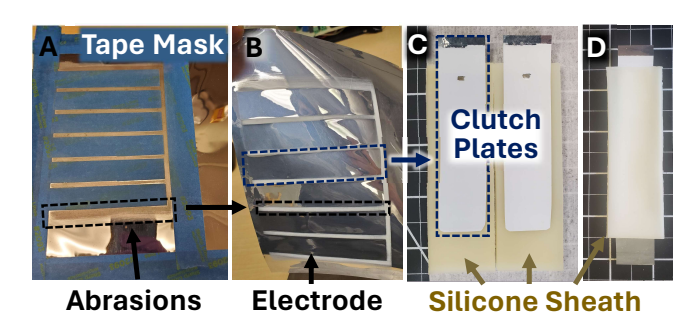


Fig. 2: Clutch fabrication process: A. Masking and abrading the aluminum-sputtered BOPET. B. Resulting clutch sheet ready to be cut (back of sheet). C. Cut clutch plates on silicone sheathing with holes for adhesive contact. D. Assembled sheathed clutch.

B. Clutch Fabrication

We implement the clutch fabrication process from [21] with an added abrasion step to remove metallization at the edges of the clutch to prevent shorting across the edges of the plates. We apply painter's tape (blue in Fig. 2A) to the active electrode regions and abrade the aluminum from the surrounding BOPET with a Scotch-Brite pad. We then coat a $25\mu m$ film of Dupont Luxprint 8153 over the entire sheet. After curing, the clutch areas are clearly distinguishable and ready to be cut (see Fig. 2B). We apply copper tape directly to the edges of clutch electrodes that remain free of Luxprint to make electrical connections to the clutch.

C. System Synthesis

We mold two rectangular pieces of silicone per system, one for each clutch plate. We adhere the clutch plates to their respective silicone near the exposed electrode, with most of the clutch plate free to slide relative to the silicone. Once the adhesive has cured, we scrape a small area of Luxprint and aluminum off the clutch plate to expose the BOPET underneath (Fig. 2C). A thin layer of adhesive is applied to this exposed BOPET and the nearby silicone for each plate. These areas are then adhered to the exposed silicone of the other piece, creating a sandwich as seen in Fig. 1.

After curing, we seal the two pieces of silicone around the remainder of their circumference with a thin layer of Sil-Poxy to keep contaminants away from the clutch plates.

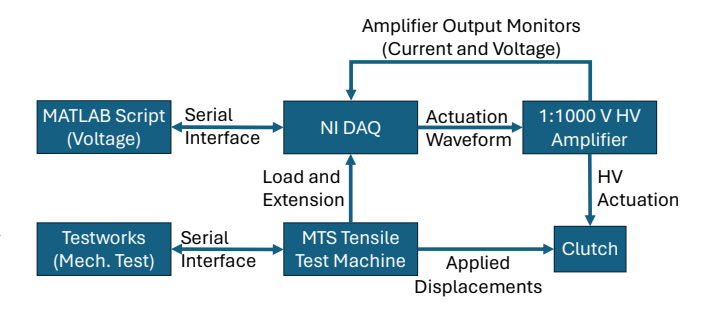


Fig. 3: Clutch Control: Block diagram of electrical control for simultaneous high-voltage PWM and tensile testing

D. PWM Clutch Control

The clutches are powered with a bipolar 300V amplitude square wave, and pulse-width modulation is applied to that square wave to create an actuation waveform (Fig. 5 inset). This waveform is calculated in MATLAB, which interacts with a National Instruments (NI) Data Acquisition (DAQ) system via serial communication. That NI DAQ creates the electronic waveform, which is then amplified 1000 fold by a high volt (HV) amplifier before reaching the clutch plates. This process, and its use in the material testing shown in Fig. 4, is represented by the block diagram in Fig. 3.

IV. SHEATHED CLUTCH CHARACTERIZATION

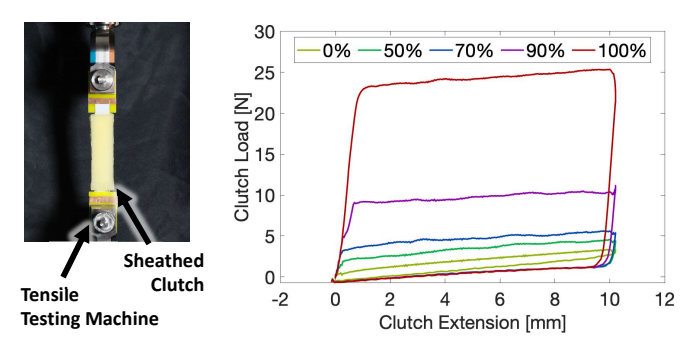


Fig. 4: (left) Experimental setup for clutch force characterization. (right) Clutch force response during loading and unloading at various PWM duty cycles (duty cycle indicated by color).

The variance between on-state and off-state force-displacement relations is measured by testing the system in a uniaxial test system (MTS Criterion). The clutches are adhered to acrylic plates, which are mechanically clamped to the MTS. Clutches are activated with the high-voltage input and then pulled at a constant rate of 250mm/min. Displacement continues as the system slips and reaches a steady-state force (subtracting the force contributed by the sheathing). When the system reaches a displacement of 10mm, the clutch is unloaded at 250 mm/min back to its original length. By comparing this force-displacement curve

(Fig. 4) to the force-displacement curve of a deactivated clutch, we isolate the component of the system load borne by the clutch, and can thus measure the clutch holding force.

In a full-power loading at 300V, the maximum tensile holding force of the clutch system reaches about 25N. At this extension, 10mm, the sheathing contributes approximately 3N and the clutch contributes approximately 22N. While there is a theoretical decrease in holding force as the clutch plates move past one other (decrease *A* in Eq. 1), the positive slope of the load-extension curve throughout loading in Fig. 4 implies that the stress of the silicone contributes more force than the clutch loses over the tested range.

We determine the empirical relationship between activation duty cycle and holding force (ζ in Eq. 3) for each PWM duty cycle ranging from 0 to 100% in increments of 10%. Example cycles with incrementally increasing duty cycles are shown in Fig. 4. The holding force was found to vary non-linearly with activation duty cycle, as seen in Fig. 5.

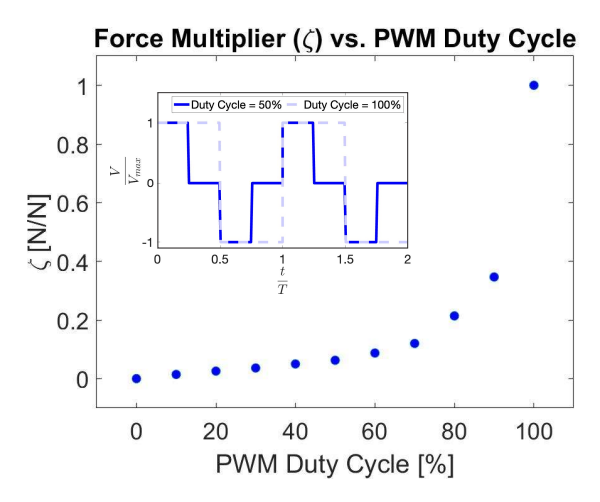


Fig. 5: Empirical relation between clutch force multiplier from Eq. 3 (ζ) and PWM duty cycle. (inset) Example waveform for PWM output at 50% and 100% duty cycle.

V. APPLICATIONS

A. Variable Non-conservative Energy Dissipation

and empirical modeling, we test the clutch in a highly constrained, highly dynamic catching task. We constructed a 1 degree-of-freedom (DoF) test stage that is restrained against gravity by two sheathed clutches. The clutches are aligned such that the stage DoF is out-of-plane from the clutch plates. The clutch systems dissipate energy throughout the motion of the stage. Modulating this energy dissipation alters the distance through which the stage drops during a catch. The sheathing is pre-tensioned by the weight of the stage (~700g), bringing the system to an initial steady state. We use two 3mm thick pieces of Ecoflex 00-30 for the sheathing such that they provide enough tensile force to minimize initial clutch system elongation and thereby maintain clutch overlap area.

We drop a 200g mass onto the stage from a height of 200mm and measure the displacement of the stage in the room's reference frame using a VICON motion-capture

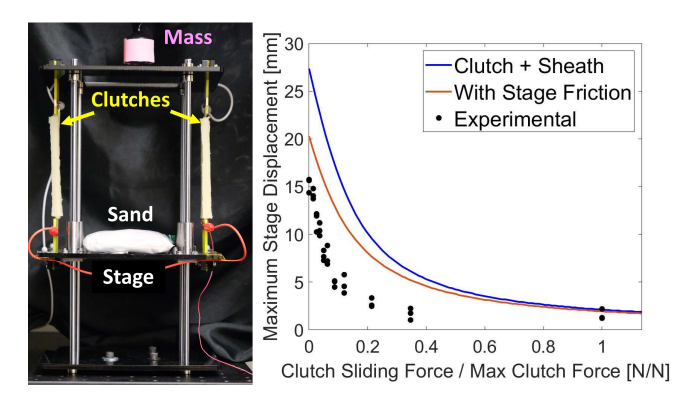


Fig. 6: (left) Experimental setup for dynamic energy dissipation with sheathed clutch. (right) Maximum stage vertical displacement as a function of clutch activation force as modeled via energy methods (Eq. 4, lines) and seen in experimental results (points). The blue line estimates dynamic response based on modeling of the clutch and sheath, while the orange line adds the work done by a constant force stage friction.

system. Displacement is measured relative to the position of the stage when the mass is dropped with downward as positive. The mass lands on a bag of microsphere sand to ensure that it remains in contact with the stage. Three trials are preformed for different activation duty cycles of the clutch system, ranging from 0% to 100% duty in increments of 10%.

2) Modeling: This stage system is modeled as a simple inelastic collision (zero coefficient of restitution), where the momentum of the mass is transferred into the mass and stage as they move together after impact. With deactivated clutches, all the kinetic energy goes into the sheathing (plus system deformation and friction), which provides an underdamped, oscillatory, response. If the clutches are activated, they act as a non-conservative decelerating force whose magnitude is limited by the duty cycle of the PWM. The kinetic energy (KE) of the stage system can be described as a function of the stage's downwards displacement, d, and trends towards zero due to the nonconservative work done by the clutches and stage friction:

$$KE_{Stage} = KE_{initial} - E_{friction} - E_{sheath} - E_{clutch}$$
(4)
$$= m \cdot g \cdot h_0 \cdot \frac{m}{m_{total}} + m_{total}gd - E_{friction}$$
$$-(E_{sheath(d)} - E_{sheath(initial)}) - dF_{clutch}$$

Where m is the mass of the dropped mass, m_{total} is the sum of m with the stage mass, h_0 is the height above the stage from which the mass is dropped, g is the standard acceleration of gravity, and F_{clutch} is the product of its max clutch holding force with ζ . Energy (E) in the sheath is the integral of the sheath force, F_{sheath} , over the displacement: $E_{sheath} = \int_{d_0}^{d} F_{sheath} dz$. Published values of material constants [22] for incompressible EcoFlex 00-30 were used in sheath energy calculations such that the calculations could be used in sheath design.

The initial kinetic energy of the system is modeled as an inelastic collision, with momentum conserved. The initial kinetic energy of the mass and stage is therefore the gravitational potential energy of the mass reduced by the factor $\frac{m}{m_{total}}$ through this collision. Friction is modeled as a constant, restrictive force and estimated to be 2.5N based on system measurements.

For a damped response (no oscillation), enough energy has to be dissipated in the clutches (E_{clutch}) that the restorative force from the sheathing is less than the gravitational force of the combined mass of the stage and dropped mass (m_{total}) when the energy (Eq. 4) reaches zero ($0 \ge F_Z = F_{sheath} - m_{total}g$). F_{sheath} can be directly calculated from the corresponding principal stress (Eq. 2) and cross-sectional area A: $F_{sheath} = \sigma_{11}A$.

This is critically different from a regular damped response in that the restorative force doesn't have to go to zero for the system to stop. Because F_{clutch} is not dependent on velocity, the system stops without oscillation so long as $-F_{clutch} < F_Z \le 0$ and Eq. 4 = 0.

3) Results: The experimental stage consistently displaces less than predicted by theory. This is, in part, due to forms of energy dissipation not included in our model such as the viscous energy losses in the silicone and stage bearings. We also fail to take into account elastic energy in the cured Sil-Poxy adhesive. Still, the general trend between force and displacement matches, as seen in Fig. 6.

Oscillations occurred in all three trials for duty cycles less than or equal to 40%. They were by far the most pronounced for 0% and 10%, which oscillated above the starting position (in all three 0% trials and one 10% trial). Oscillations also occurred in one trial at 50% and one trial at 70%. Theory predicts oscillations ($F_Z > 0$) at normalized clutch forces below ~ 0.32 , which is consistent with a duty cycle between 80% and 90% based on our initial characterization.

B. SPA Strain Limitation

1) SPA Fabrication & Experimental Setup: To test the strain limitation potential of the sheathed clutch, we attached it to a low-pressure, silicone, inverse pneumatic artificial muscle (IPAM). We injection-molded the body of the IPAM with EcoFlex 00-30 in a 3d-printed mold to create a cylinder with wall thicknesses of 1.5mm. After it cured, we wrapped inextensible fiber (Power Pro 40lb braided line) around the body by rotating the silicone on a drill, similar to [23]. We secured the fiber to the body at both ends with Sil-Poxy and cast an additional, thin, layer of EcoFlex 00-30 on top of the fibers by blade-casting while the system rotates. The system was left spinning during curing to provide even distribution of silicone. Finally, we used Sil-Poxy to adhere a harder silicone (Smooth-Sil 936) to the flat of the cylinder as a cap.

The sheathing is made of two 1.5mm thick pieces of Ecoflex 00-30 to minimize off-state antagonistic forces. To adhere the sheathed clutches to the IPAM, we use Sil-Poxy along the entire area of the sheath. We secured the sheath to the IPAM with zip-ties during curing to ensure conformal contact. After curing, we attached a second clutch system to the opposite side in the same manner to balance out

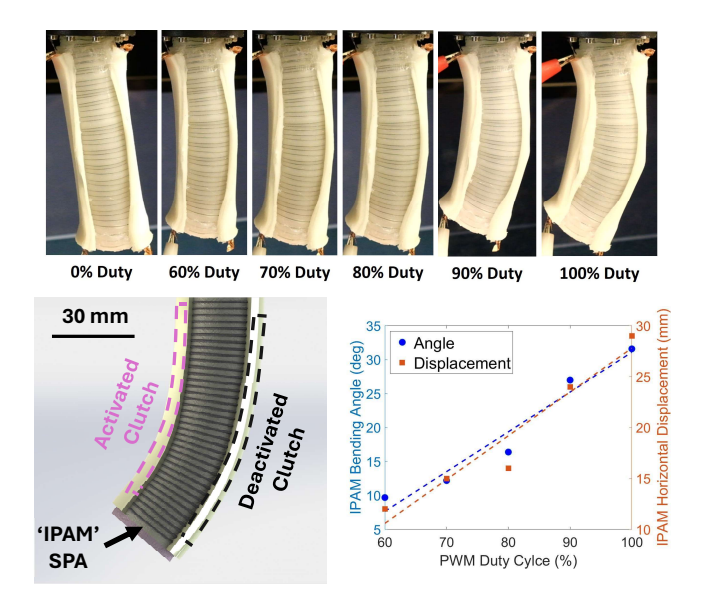


Fig. 7: (top) SPA inflated to approximately 25 kPa with different clutch duty cycles. (left) Diagram of SPA expansion with fully activated clutch. (right) PWM effect on bending angle and horizontal displacement.

the sheath's passive constraint and allow for single-DoF extension when clutches are inactive.

We actuate the IPAM with a 6V DC pump to an internal gauge pressure of 25 kPa, which we monitor via a Qwiic MicroPressure sensor in a connected pressure chamber. Immediately prior to and throughout actuation, we activate one of the two sheathed clutches to duty cycles corresponding to the characterized values in Fig. 5. We record the extension with a head-on view. Video frames are used to determine pressure at which the clutch transitions from a static hold to a stick-slip regime, as well as the bending angle and horizontal position at 25 kPa (Digimizer 6.3.0).

2) Results: Low duty cycles, below 60%, had a minimal effect on the trajectory of the SPA. Starting at 60% duty cycle, there was a direct correlation between clutch holding force and the pressure at which it slipped. The clutches began slipping at the following pressures for 60-100% duty cycles respectively: 5, 6, 7, 10, 15 kPa.

Slipping allows for the clutch system to stretch while still applying an antagonistic force throughout inflation. Once we held internal pressure constant at 25kPa, slipping no long occurred and there was a unique bending angle and horizontal position for each duty cycle. We will consider bending angle of the IPAM as the clockwise angle from the base plate to the cap. The horizontal displacement of the center of the IPAM cap is measured relative to the position with an inactive clutch. Measurements are taken horizontally in a reference frame fixed at the mount with leftward motion as positive. Zero is considered as the angle or displacement of the IPAM at 25kPa with the left clutch completely inactive. The right clutch is never activated. Results for angle and displacement are seen in Fig. 7 with linear trend lines.

The strain-limiting ability of the sheathed clutch is variable in that it slips and then continues to limit strain at a different length. The relation between SPA internal pressure and clutch stress after slip is therefore complex and its exploration is left for future work.

VI. CONCLUSIONS AND FUTURE WORK

This work presents design and fabrication techniques for a clutch system that is directly useful for antagonistic forces in soft pneumatic actuation. We calculate off-state constitutive response for sheathing design, and relate active force control to PWM electrical inputs. The system functions in accordance with modeling expectations in the dynamic catching demonstration. We then show how PWM of a clutch can control the effective stiffness of a material to enable position control of the end point of an IPAM actuator.

Future work is required to better characterize PWM control of on-state electrostatic adhesion. We will aim to develop a theoretical understanding of the empirical relations found in [17] and Fig 5. Though the shape of the relation is similar to a quadratic that we would expect from a voltage change, there appears to be a lesser holding force associated with the modulation. Further modeling of the effect of this mode of strain limitation on a SPA would also be helpful in determining the best use-cases.

There is significant potential for augmenting SPA trajectory and force outputs with this clutch system. Beyond the shape morphing shown previously [12], the use of these antagonistic systems can theoretically increase force output for SPAs and enable large-scale object manipulation. Modeling advances for the combined soft system will likely be required to enable these modalities. We also hope to expand the versatility of the system by adding repeatable external adhesion to the clutch system, similar to [5]. Further work improving the holding performance of EA clutches will also enable higher-pressure SPA applications.

ACKNOWLEDGMENT

This work was supported in part by National Science Foundation (NSF) Emerging Frontiers in Research and Innovation (EFRI) award #1935294 and NSF Research Traineeship (NRT) award #2152205.

REFERENCES

- R. F. Shepherd, F. Ilievski, W. Choi, et al., "Multigait soft robot," Proceedings of the National Academy of Sciences, vol. 108, no. 51, pp. 20400–20403, 2011.
- [2] B. Mosadegh, P. Polygerinos, C. Keplinger, et al., "Pneumatic networks for soft robotics that actuate rapidly," Advanced Functional Materials, vol. 24, no. 15, pp. 2163–2170, 2014.
- [3] J. Pikul, S. Li, H. Bai, R. Hanlon, I. Cohen, and R. Shepherd, "Stretchable surfaces with programmable 3d texture morphing for synthetic camouflaging skins," *Science*, vol. 358, no. 6360, pp. 210– 214, 2017.
- [4] N. Sholl, A. Moss, M. Krieg, and K. Mohseni, "Controlling the deformation space of soft membranes using fiber reinforcement," *The International Journal of Robotics Research*, vol. 40, no. 1, pp. 178–196, 2021.
- [5] S. Y. Kim, R. Baines, J. Booth, N. Vasios, K. Bertoldi, and R. Kramer-Bottiglio, "Reconfigurable soft body trajectories using unidirectionally stretchable composite laminae," *Nature Communi*cations, vol. 10, no. 1, pp. 1–8, 2019.

- [6] B. Yang, R. Baines, D. Shah, et al., "Reprogrammable soft actuation and shape-shifting via tensile jamming," Science Advances, vol. 7, no. 40, eabh2073, 2021.
- [7] A. Firouzeh, M. Salerno, and J. Paik, "Soft pneumatic actuator with adjustable stiffness layers for multi-dof actuation," in 2015 IEEE/RSJ International Conference on Intelligent Robots and Systems (IROS), IEEE, 2015, pp. 1117–1124.
- [8] J.-Y. Lee, E.-Y. Go, W.-Y. Choi, W.-B. Kim, and K.-J. Cho, "Development of soft continuum manipulator with pneumatic and tendon driven actuations," in 2016 13th International Conference on Ubiquitous Robots and Ambient Intelligence (URAI), IEEE, 2016, pp. 377–379.
- [9] K. C. Galloway, P. Polygerinos, C. J. Walsh, and R. J. Wood, "Mechanically programmable bend radius for fiber-reinforced soft actuators," in 2013 16th International Conference on Advanced Robotics (ICAR), 2013, pp. 1–6.
- [10] A. Sedal, M. Fisher, J. Bishop-Moser, A. Wineman, and S. Kota, "Auxetic sleeves for soft actuators with kinematically varied surfaces," in 2018 IEEE/RSJ International Conference on Intelligent Robots and Systems (IROS), 2018, pp. 464–471.
- [11] M. R. Devlin, B. T. Young, N. D. Naclerio, D. A. Haggerty, and E. W. Hawkes, "An untethered soft cellular robot with variable volume, friction, and unit-to-unit cohesion," in 2020 IEEE/RSJ International Conference on Intelligent Robots and Systems (IROS), IEEE, 2020, pp. 3333–3339.
- [12] G. M. Campbell, J. Yin, Y. Song, U. Gandhi, M. Yim, and J. Pikul, "Electroadhesive clutches for programmable shape morphing of soft actuators," in 2022 IEEE/RSJ International Conference on Intelligent Robots and Systems (IROS), IEEE, 2022, pp. 11594–11599.
- [13] D. J. Levine, K. T. Turner, and J. H. Pikul, "Materials with electroprogrammable stiffness," *Advanced Materials*, p. 2007 952, 2021
- [14] S. B. Diller, S. H. Collins, and C. Majidi, "The effects of electroadhesive clutch design parameters on performance characteristics," *Journal of Intelligent Material Systems and Structures*, vol. 29, no. 19, pp. 3804–3828, 2018.
- [15] R. Hinchet and H. Shea, "High force density textile electrostatic clutch," *Advanced Materials Technologies*, vol. 5, no. 4, p. 1900 895, 2020.
- [16] R. J. Hinchet and H. Shea, "Glove-and sleeve-format variable-friction electrostatic clutches for kinesthetic haptics," *Advanced Intelligent Systems*, vol. 4, no. 12, p. 2 200 174, 2022.
- [17] N. Feizi, S. F. Atashzar, M. R. Kermani, and R. V. Patel, "Modeling and high-definition control of a smart electroadhesive actuator: Toward application in rehabilitation," *IEEE Transactions on Medical Robotics and Bionics*, vol. 4, no. 4, pp. 1057–1067, 2022.
- [18] D. J. Levine, G. M. Iyer, R. D. Roosa, K. T. Turner, and J. H. Pikul, "A mechanics-based approach to realize high-force capacity electroadhesives for robots," *Science Robotics*, vol. 7, no. 72, eabo2179, 2022.
- [19] A. N. Gent, "A new constitutive relation for rubber," Rubber Chemistry and Technology, vol. 69, no. 1, pp. 59–61, 1996.
- [20] Y. Sun, K. M. Digumarti, H.-V. Phan, O. Aloui, and D. Floreano, "Electro-adhesive tubular clutch for variable-stiffness robots," in 2022 IEEE/RSJ International Conference on Intelligent Robots and Systems (IROS), IEEE, 2022, pp. 9628–9634.
- [21] S. Diller, C. Majidi, and S. H. Collins, "A lightweight, low-power electroadhesive clutch and spring for exoskeleton actuation," in 2016 IEEE International Conference on Robotics and Automation (ICRA), IEEE, 2016, pp. 682–689.
- [22] D. Steck, J. Qu, S. B. Kordmahale, D. Tscharnuter, A. Muliana, and J. Kameoka, "Mechanical responses of ecoflex silicone rubber: Compressible and incompressible behaviors," *Journal of Applied Polymer Science*, vol. 136, no. 5, p. 47025, 2019.
- [23] E. W. Hawkes, D. L. Christensen, and A. M. Okamura, "Design and implementation of a 300% strain soft artificial muscle," in 2016 IEEE International Conference on Robotics and Automation (ICRA), IEEE, 2016, pp. 4022–4029.